Dalton Transactions

PAPER

View Article Online
View Journal | View Issue

Cite this: *Dalton Trans.*, 2015, **44**, 14042

Heteroleptic strontium complexes stabilized by donor-functionalized alkoxide and β-diketonate ligands†

Sheby Mary George,[a] Hyo-Suk Kim,[a] Hyun Ji Oh,[a] Myoung Soo Lah,[b] Dong Ju Jeon,[a] Bo Keun Park,[a] Jeong Hwan Han,[a] Chang Gyoun Kim*[a] and Taek-Mo Chung*[a]

Heteroleptic complexes of strontium (**1–7**) were prepared by employing β-diketonates and donor-functionalized alkoxides as coordinating ligands. The results illustrate the effect of alkoxide substituent groups on the overall structures of the complexes. The presence of a terminal methoxy group in the alkoxide ligands leads to the formation of trimeric complexes **1–4**, whereas the substituents on the amine nitrogen prove to have less influence in determining the structure. The attempts to increase steric bulkiness of the aminoalkoxide ligands by introducing ethyl groups on the amine nitrogen and to the alkoxy carbon did not lead to a structural change from the dimeric form in **5–7** but resulted in structurally interesting strontium complexes. In trimeric complexes **2–4**, the three strontium atoms were held together by two μ_3-O bonds using alkoxide oxygen atoms and two μ_2-O bonds using a combination of alkoxide and β-diketonate ligand oxygens. The strontium metal centers in these complexes exhibit seven-coordination states in **2** and **4**, whereas **3** exhibits one six-coordinated and two seven-coordinated strontium metals in its structure. All of the complexes were characterized using FT-NMR, FT-IR, elemental analyses, and thermogravimetric (TG) analyses.

Received 10th April 2015,
Accepted 25th June 2015

DOI: 10.1039/c5dt01356a

www.rsc.org/dalton

Introduction

The applications in the semiconductor industry and in catalysis are the driving forces for the large interest in group 2 metal chemistry. Among these, strontium compounds have a key role in electronics due to the importance of strontium containing metal oxides.[1] These applications largely depend on the fabrication of strontium containing metal oxide thin films preferably through atomic layer deposition (ALD) or chemical vapor deposition (CVD). For the deposition of thin films using these techniques, strontium precursors with good stability and volatility are essential. However, the large ionic radii and relatively small charge (+2) associated with strontium ions make the development of volatile precursors with suitable properties a challenge. In the past, the formation of unfavorable oligomeric compounds has been viewed as a main challenge, but that has been solved by using multi-dentate, sterically bulky ligands that form strong bonds with strontium.[2] However, the achievements in the development of volatile strontium precursors did not ensure their successful application in the thin film industry because of several factors such as instability, unwanted side reactions, and carbon contamination in films. These unfavorable factors associated with the existing precursors forced researchers to continue the development of new and better strontium complexes to satisfy the industry requirements.

The most common method to develop a new precursor is using a newly designed ligand, or modifying the existing ligands by introducing functionalities to satisfy the needs. The development of an entirely new ligand system is not only a time consuming process but also does not ensure success. At this point, recent developments in heteroleptic precursor chemistry and its application are gaining importance.[3] The heteroleptic metal precursors, where the central metal atom is bonded to different types of ligands, have a distinct advantage of having a different dissociation pattern for each ligand, which might be useful in the development of thin films. Even though the development of heteroleptic metal precursors faces similar challenges to those of homoleptic metal precursors

[a]*Thin Film Materials Research Center, Korea Research Institute of Chemical Technology, P.O. Box 107, 141 Gajeong-Ro, Yuseong-Gu, Daejeon 305-600, Republic of Korea. E-mail: cgkim@krict.re.kr, tmchung@krict.re.kr; Fax: (+82)42-861-4151*
[b]*Interdisciplinary School of Green Energy, Ulsan National University of Science and Technology, UNIST-gil 50, Ulsan 689-798, Republic of Korea*

† Electronic supplementary information (ESI) available: ORTEP diagrams of complexes **5** and **6**, selected bond angles of complexes **2–4**, and the VT-NMR plots of complexes **1**, **5**, and **7**. CCDC 1034384–1034389 for **2–7**. For ESI and crystallographic data in CIF or other electronic format see DOI: 10.1039/c5dt01356a

and depends on the selection of suitable combinations of ligands, it can lead to much better results than those of homoleptic complexes.[3,4] The availability of a large known ligand pool from which to select ligands and the research results of their homoleptic precursors make the development of heteroleptic metal precursors much easier.

Our recent results of a heteroleptic strontium complex $[Sr(demamp)(tmhd)]_2$ (**8**)[4] with 1-{[2-(dimethylamino)ethyl](methyl)amino}-2-methylpropan-2-olate (demamp) and 2,2,6,6-tetramethyl-3,5-heptanedionate (tmhd) as coordinating ligands and superior physical properties to homoleptic complexes encouraged us to conduct further research into this class of strontium complexes. The simple preparation of [Sr(β-diketonate)(aminoalkoxide)] complexes by controlled substitution on strontium bis(trimethylsilyl)amides ($Sr(btsa)_2$), stability in various coordinating solvents as well as at high temperatures, and commercial availability or simple preparative methods of the ligands are attractions of this class of complexes. The good volatility and stability of the above complex overcame the common drawbacks of dimeric/oligomeric structures, and the dimeric structure proved to be the stable form for this class of complexes. Here in this paper we further studied the structures and properties of this class of complexes using potential tridentate donor-functionalized alkoxides in combination with β-diketonate ligands. The results of the chemistry and structural investigations of the new complexes are described in this paper.

Results and discussion

In this work, we introduced a variety of potential tridentate ligands to study the effect of steric groups on coordinating heteroatoms on the complex structure and its properties. The tridentate ligands used (Table 1) in this work were 1-((2-methoxyethyl)(methyl)amino)-2-methylpropan-2-ol (memampH) for **1**, 1-(ethyl(2-methoxyethyl)amino)-2-methylpropan-2-ol (emeampH) for **2**, 1-(isopropyl(2-methoxyethyl)amino)-2-methylpropan-2-ol (imeampH) for **3**, 1-(2-methoxyethoxy)-2-methylpropan-2-ol (mempH) for **4**, 1-((2-(dimethylamino)ethyl)(ethyl)amino)-2-methylpropan-2-ol (dmaeeampH) for **5**, 1-((2-(dimethylamino)ethyl)(methyl)amino)-2-methylbutan-2-ol (dmaemambH) for **6** and 3-(((2-(dimethylamino)ethyl)(methyl)-amino)methyl)pentan-3-ol (dmaemampH) for **7**. In complexes **1–6**, 2,2,6,6-tetramethyl-3,5-heptanedione (tmhdH) was used as a β-diketonate ligand whereas 2,6-dimethyl-3,5-heptanedione (dmhdH) was used in **7**. The tridentate memampH, emeampH, and imeampH ligands were introduced to investigate the effect of a terminal methoxy group in place of an amine group as well as the effect of progressively increased bulkiness on the tertiary amine groups in these ligands with respect to the demampH ligand. The mempH was introduced as a simple ligand with far less steric hindrance on the coordinating sites. The dmaeeampH and dmaemambH ligands were intended to test the stable dimeric structures of this class of complexes by increasing bulkiness and introducing chirality, whereas the dmaemampH/dmhdH combination was used to produce a complex that is molecularly similar to **8**.

Table 1 List of ligands used in complexes **1–7**

Complex	Ligand	Ligand structure
1	memampH	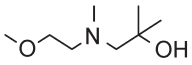
2	emeampH	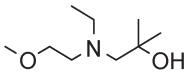
3	imeampH	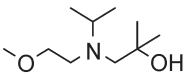
4	mempH	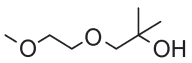
5	dmaeeampH	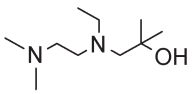
6	dmaemambH	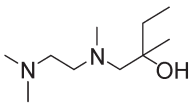
7	dmaemampH	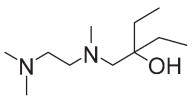

The complexes were prepared through a procedure similar to that reported previously.[5] The $Sr[N(SiMe_3)_2]_2{\cdot}2DME$ solution in toluene was first treated with the corresponding alcohol in an equivalent ratio followed by the addition of tmhdH or dmhdH (as shown in Scheme 1), and the resulting reaction mixture was stirred overnight at room temperature to afford the respective complexes **1–7**. The X-ray quality crystals of complexes **2–7** were grown from saturated hexane solutions of the corresponding complexes at −30 °C. Efforts to make single crystals of compound **1** resulted in needle type crystals that were not suited for structural analysis.

Crystal structure

The results obtained from the single-crystal structural analyses showed that complexes **2–4** crystallized as trimers, whereas complexes **5–7** displayed dimeric structures (Table 2). Complex **2**, which crystallized in a triclinic $P\bar{1}$ (Fig. 1) space group, exhibits heptacoordinated strontium metal centers. The strontium atoms are directly bonded to one emeamp and one tmhd ligand each, and the three [Sr(emeamp)(tmhd)] fractions are held together by a combination of μ_2- and μ_3-oxygen bridging between the metal atoms. The emeamp ligands attached to Sr1 and Sr2 undergo μ_3-oxygen bridging with all three strontium atoms through the alkoxide oxygen atoms, whereas the emeamp ligand attached to Sr3 engages in μ_2-oxygen bridging with the neighboring Sr1. The μ_2-O bridging of the tmhd oxygen attached to Sr3 with Sr1 completes the metal–O–metal network. Complex **3** which crystallized in a similar triclinic $P\bar{1}$

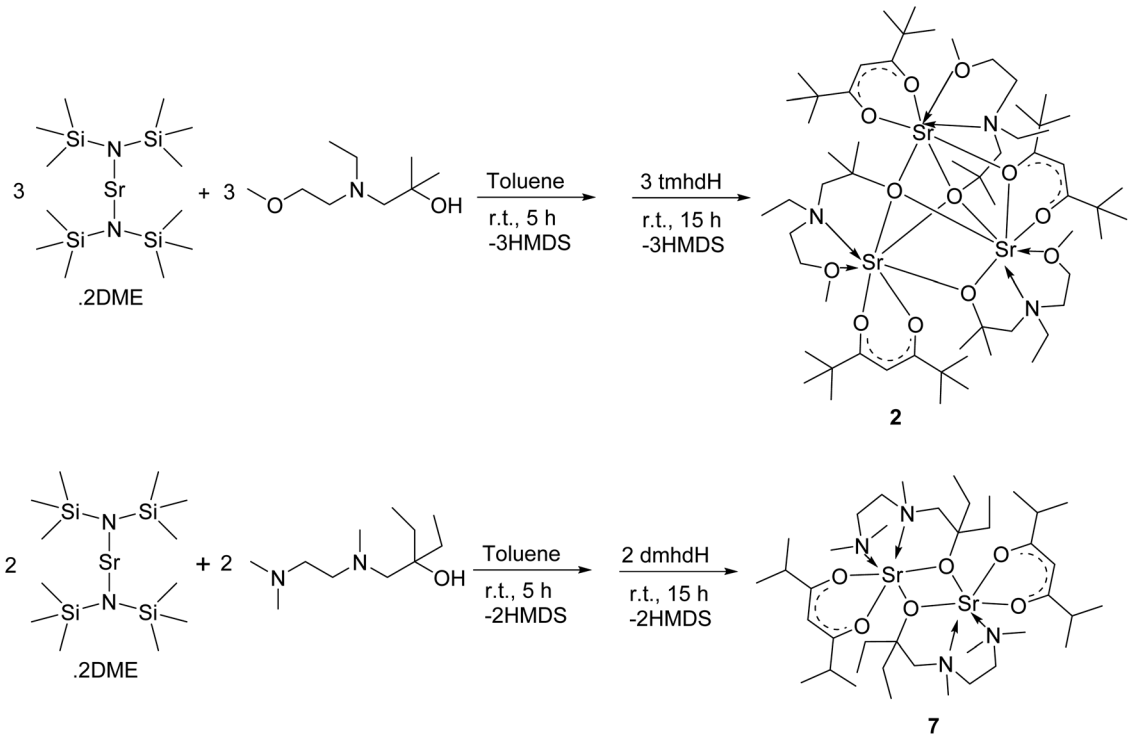

Scheme 1 Synthesis of complexes **2** and **7**.

Table 2 Crystallographic data and data collection parameters for **2–7**

Compound	(**2**)	(**3**)	(**4**·0.5 Hex)	(**5**)	(**6**)	(**7**)
Formula weight	1335.42	1377.50	1297.30	916.37	916.37	888.32
Temperature (K)	100(1)	100(1)	100(1)	100(1)	100(1)	100(1)
Wavelength (Å)	0.71073	0.71073	0.71073	0.71073	0.71073	0.71073
Crystal system	Triclinic	Triclinic	Triclinic	Monoclinic	Monoclinic	Triclinic
Space group	$P\bar{1}$	$P\bar{1}$	$P\bar{1}$	$P2(1)/c$	$P2(1)/n$	$P\bar{1}$
a (Å)	14.9083(2)	14.1918(2)	10.6143(5)	10.6303(2)	9.8488(3)	10.7509(4)
b (Å)	15.5225(2)	14.5190(2)	16.2868(7)	22.0103(4)	25.0965(7)	15.1148(6)
c (Å)	17.1464(2)	21.0895(3)	21.4751(10)	11.6362(2)	10.1883(3)	16.3750(7)
α (°)	78.9340(10)	77.3070(10)	94.454(3)	90°	90°	93.525(2)
β (°)	85.2550(10)	71.7630(10)	103.164(2)	112.8670(10)	101.478(2)	105.381(2)
γ (°)	63.5860(10)	63.7730(10)	106.686(2)	90°	90°	108.420(2)
V (Å^3)	3487.59(8)	3685.39(9)	3421.7(3)	2508.62(8)	2467.88(13)	2403.25(17)
Z	6	2	2	2	2	2
ρ_{calcd} (Mg m^{-3})	1.272	1.241	1.259	1.213	1.233	1.228
μ (mm^{-1})	2.340	2.217	2.385	2.169	2.205	2.262
F(000)	1416	1464	1370	976	976	944
Crystal size (mm^3)	0.20 × 0.16 × 0.08	0.10 × 0.08 × 0.06	0.16 × 0.12 × 0.06	0.16 × 0.12 × 0.10	0.10 × 0.08 × 0.06	0.25 × 0.25 × 0.22
Theta range for data collection (°)	1.21 to 28.23	1.57 to 28.31	0.99 to 28.33	1.85 to 28.31	1.62 to 28.36	1.44 to 28.39
Index ranges	$-19 \le h \le 19$, $-20 \le k \le 20$, $0 \le l \le 22$	$-17 \le h \le 18$, $-18 \le k \le 19$, $0 \le l \le 28$	$-14 \le h \le 13$, $-21 \le k \le 21$, $0 \le l \le 28$	$-14 \le h \le 13$, $0 \le k \le 29$, $0 \le l \le 15$	$-13 \le h \le 12$, $0 \le k \le 33$, $0 \le l \le 13$	$-14 \le h \le 14$, $-20 \le k \le 20$, $-21 \le l \le 21$
Total reflns	17 151	18 256	16 978	6241	6133	62 066
Independent reflns (R_{int})	17 151 (0.00)	18 256 (0.00)	16 978(0.00)	6241 (0.00)	6133(0.00)	11 941 (0.0545)
Parameters	703	731	685	253	244	469
GOF on F^2	1.032	1.020	1.031	1.036	1.022	1.225
R_1 [$I > 2\sigma(I)$]	0.0462	0.0623	0.0434	0.0370	0.0486	0.0612
wR_2 [$I > 2\sigma(I)$]	0.0770	0.1179	0.0838	0.0758	0.1071	0.1602

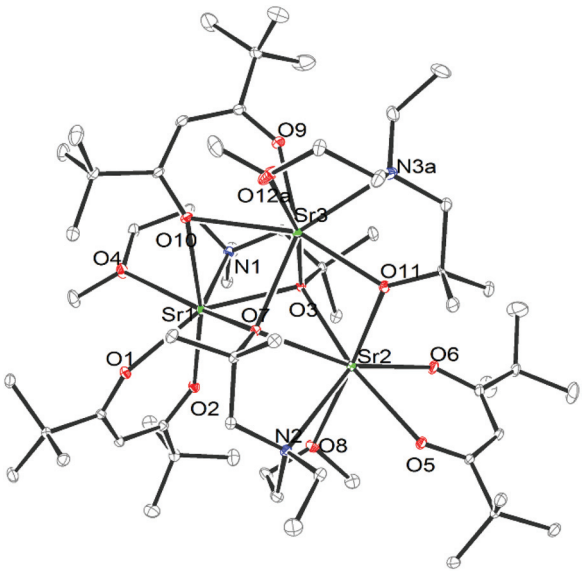

Fig. 1 ORTEP diagram for complex 2.

space group (Fig. 2), exhibits one hexacoordinated and two heptacoordinated metal centers in its trimeric structure. Unlike **2**, the metal–O–metal network in **3** consists of two μ_3-oxygen bridges and three μ_2-oxygen bridges. Of the two imeamp ligands that undergo μ_3-oxygen bridging in **3**, one is bonded to Sr2 utilizing all three available coordination sites whereas the other displays an uncoordinated amine group and an ether group. The steric interaction between the isopropyl moieties attached to the amine nitrogen in imeamp and that of the *tert*-butyl group of tmhd might have made the complete coordination of imeamp with Sr1 impossible, leaving Sr1 in a hexacoordinated state. To complete its coordination, Sr1 undergoes μ_2-O bridging with Sr3 through the imeamp ligand attached to Sr3 and μ_2-O bridging with Sr2 through the tmhd ligand attached to Sr2. The μ_2-O bridging of a tmhd oxygen atom from Sr3 with Sr2 completes the metal–O–metal bonding in **3**. Complex **4** (Fig. 3), which crystallized as a trimeric complex in a triclinic $P\bar{1}$ space group, exhibits structural similarity to **2**. In a very similar fashion to **2**, all three metal centers are connected through μ_3-oxygen bridging using the alkoxide oxygens of two memp ligands. The μ_2-O bridge between Sr1 and Sr2 is formed using an memp alkoxide O-atom and that between Sr2 and Sr3 is formed using a tmhd O-atom. Complexes **5–7**, where the aminoalkoxide ligands exerted more steric hindrance than in the above described complexes because of the presence of terminal amine groups, crystallized as dimers following a common trend in this class of compounds. The metal centers in these complexes exhibit hexacoordinated, distorted octahedral structures and the two metal centers are connected by two μ_2-O bonds with the alkoxide oxygen atoms from the alkoxide ligands.

The crystal structures of complexes **2–4** show that the presence of the terminal methoxy groups in the emeamp, imeamp, and memp ligands decreases the steric hindrance exerted by these ligands with respect to demamp in $[Sr(demamp)(tmhd)]_2$ (**8**) and results in the formation of trimeric structures. The ethyl group on the amine nitrogen in emeamp did not show much influence on the structure of **2**, whereas the isopropyl group in the imeamp ligand had an influence on the structure of **3**. The imeamp ligand attached to Sr1 experienced strong steric interactions from the tmhd *tert*-butyl group, which forced imeamp to adopt a position that prevented coordination of the amine nitrogen and the terminal methoxy group

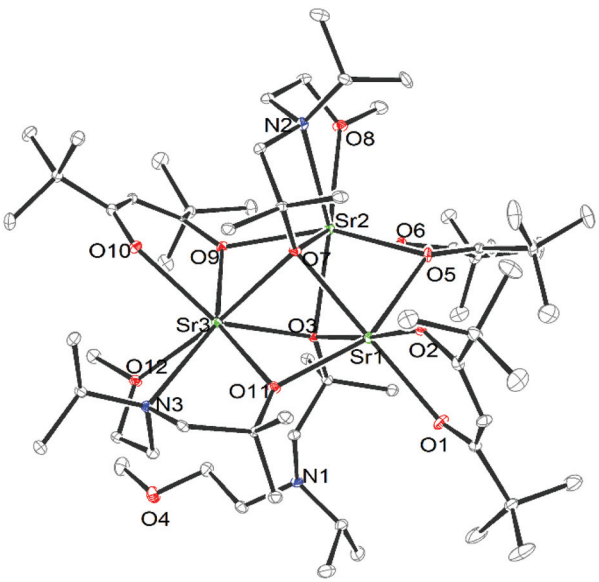

Fig. 2 ORTEP diagram for complex 3.

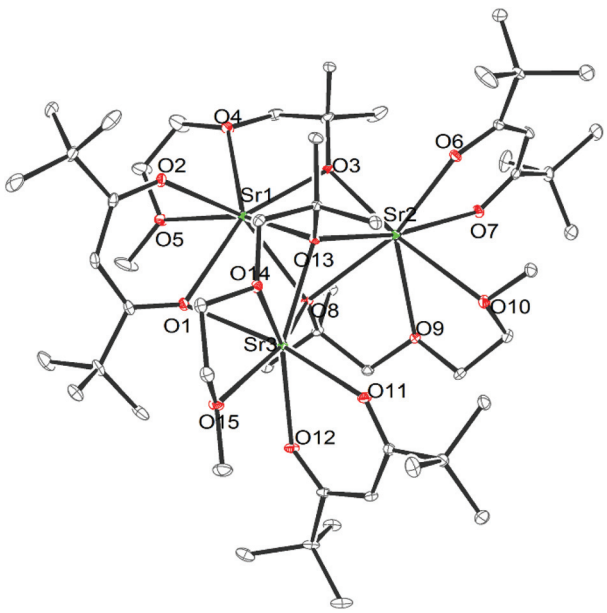

Fig. 3 ORTEP diagram for complex 4.

with a strontium ion. This caused Sr1 to appear as the sole hexacoordinated metal center in all trimeric complexes. The memp ligand in complex **4** (Fig. 3) with only oxygen-based coordination sites poses fewer steric interactions with the neighboring groups and forms a trimeric complex isostructural with **2**. The metal–metal nonbonding distances (Table 3) of Sr2···Sr3 3.6273(5) and Sr1···Sr3 3.5256(5) Å in **2** and Sr2···Sr1 3.5566(4) Å and Sr1···Sr3 3.6067(4) Å in **4** were comparable to those in a similarly bonded complex $[Sr_3(tmhd)_3(O\text{-}SiPh_3)_3]$[6] (average Sr···Sr is (3.588(2) Å), and these strontium pairs were each connected through three oxygen bridges. On the other hand the Sr1···Sr2 in **2** and Sr2···Sr3 in **4** paired by only two sets of O-bridges show longer metal–metal distances of 4.0468(5) and 3.9997(4) Å, respectively and these were still longer than the similarly paired Sr···Sr in $[Sr(thd)_2]_3$[7] (average Sr···Sr is (3.8264(1) Å) where metal atoms were paired by two sets of O-bridges. In complex **3** all three metal centers were connected by three sets of O-bridges, with metal–metal nonbonding distances of Sr2···Sr3 3.6604(6), Sr1···Sr3 3.5420(6), and Sr1···Sr2 3.6298(6) Å, which were comparable to those in $[Sr_3(tmhd)_3(OSiPh_3)_3]$.[6] The strontium metal ions in **2** have distorted pentagonal–bipyramidal coordination environments where O4 and O11 occupy the axial positions with respect to Sr1, O6 and O10 with respect to Sr2, and O7 and O12 with respect to Sr3. In **3**, Sr1 has a distorted octahedral geometry, whereas Sr2 and Sr3 have pentagonal–bipyramidal structures. The bond angles (Table S1†) of O3–Sr2–O8 and O7–Sr3–O12 were 163.99(11)° and 168.43(10)°, respectively; these formed the axial bond pairs with each strontium ion. In **4**, the bond angles of O13–Sr1–O5, O7–Sr2–O13, and O11–Sr3–O1 were 164.98(6)°, 166.11(7)°, and 167.33(7)°, respectively which indicated that the respective oxygen atoms were in axial positions relative to the corresponding strontium atoms. The bonding constraints due to the μ_2/μ_3-bridging appear to be the main causes of the distortions from the idealized geometries and the bond angles involving μ_2/μ_3 oxygen atoms display sharp deviations from the ideal angles.

The Sr–O bond lengths in the above complexes vary largely from 2.401(3) to 2.749(2) Å because of the μ_2/μ_3-bridging involving oxygen atoms as well as steric interactions in the molecule. The shortest bond lengths in **2** involve the emeamp alkoxy oxygen (O11), which bridges Sr1 and Sr3 (bond lengths of 2.401(3) and 2.425(3) Å). The bonds involving μ_3-oxygen atoms in **2** display an average bond length of 2.557(2) Å. The bonds between strontium and non-bridging tmhd oxygen atoms show an average length of 2.4888(3) Å, whereas the μ_2-bridging oxygen atom of the tmhd ligand shows bond lengths of 2.611(2) (Sr2–O10) and 2.744(3) Å (Sr3–O10). The methoxy oxygens and strontium atoms form the Sr1–O4 (2.601(3) Å), Sr2–O8 (2.703(3) Å), and Sr3–O12 (2.650(3) Å) bonds, respectively. The steric interactions between the ^{t}Bu group of the tmhd ligand and the methoxy group are thought to be the main factors behind the longer bond lengths for Sr2–O8 and Sr3–O10.

In **3**, the bonds between μ_3-O atoms and strontium metal centers show an average length of 2.513(3) Å. The bonds involving tmhd μ_2-O atoms show an average bond length of 2.643(5) Å whereas, the bonds involving imeamp μ_2-O atom show bond lengths of 2.415(3) (Sr1–O11) and 2.447(3) (Sr3–O11) Å. The Sr–O bonds with non-bridging oxygen atoms of tmhd

Table 3 Selected bond lengths (Å) for **2**, **3**, and **4**

$[Sr(emeamp)(tmhd)]_3$ (**2**)		$[Sr(imeamp)(tmhd)]_3$ (**3**)		$[Sr(memp)(tmhd)]_3$ (**4**)	
Bond lengths (Å)					
Sr(1)–O(1)	2.4577(19)	Sr(1)–O(1)	2.448(3)	Sr(1)–O(1)	2.6295(19)
Sr(1)–O(2)	2.4895(19)	Sr(1)–O(2)	2.448(3)	Sr(1)–O(2)	2.484(2)
Sr(1)–O(3)	2.4977(18)	Sr(1)–O(3)	2.547(3)	Sr(1)–O(3)	2.4244(19)
Sr(1)–O(4)	2.702(2)	Sr(1)–O(5)	2.705(3)	Sr(1)–O(4)	2.624(2)
Sr(1)–O(7)	2.5433(18)	Sr(1)–O(7)	2.525(3)	Sr(1)–O(5)	2.704(2)
Sr(1)–O(10)	2.6099(19)	Sr(1)–O(11)	2.414(3)	Sr(1)–O(8)	2.504(2)
Sr(1)–N(1)	2.803(2)	Sr(2)–O(3)	2.526(3)	Sr(1)–O(13)	2.5606(18)
Sr(2)–O(3)	2.6252(18)	Sr(2)–O(5)	2.539(3)	Sr(2)–O(3)	2.399(2)
Sr(2)–O(5)	2.5178(19)	Sr(2)–O(6)	2.467(3)	Sr(2)–O(6)	2.492(2)
Sr(2)–O(6)	2.521(2)	Sr(2)–O(7)	2.456(3)	Sr(2)–O(7)	2.479(2)
Sr(2)–O(7)	2.6019(18)	Sr(2)–O(8)	2.670(3)	Sr(2)–O(8)	2.6202(18)
Sr(2)–O(8)	2.5999(19)	Sr(2)–O(9)	2.597(3)	Sr(2)–O(9)	2.667(2)
Sr(2)–O(11)	2.3986(19)	Sr(2)–N(2)	2.915(4)	Sr(2)–O(10)	2.749(2)
Sr(2)–N(2)	2.913(2)	Sr(3)–O(3)	2.540(3)	Sr(2)–O(13)	2.5498(19)
Sr(3)–O(3)	2.5417(18)	Sr(3)–O(7)	2.483(3)	Sr(3)–O(1)	2.571(2)
Sr(3)–O(7)	2.5223(18)	Sr(3)–O(9)	2.731(3)	Sr(3)–O(8)	2.5361(18)
Sr(3)–O(9)	2.456(2)	Sr(3)–O(10)	2.490(3)	Sr(3)–O(11)	2.440(2)
Sr(3)–O(10)	2.742(2)	Sr(3)–O(11)	2.447(3)	Sr(3)–O(12)	2.484(2)
Sr(3)–O(11)	2.4240(19)	Sr(3)–O(12)	2.613(3)	Sr(3)–O(13)	2.4971(19)
Sr(3)–O(12A)	2.649(2)	Sr(3)–N(3)	2.834(4)	Sr(3)–O(14)	2.661(2)
Sr(3)–N(3A)	2.870(3)			Sr(3)–O(15)	2.730(2)
Sr(2)···Sr(3)	3.5256(5)	Sr(1)···Sr(3)	3.5420(6)	Sr(1)···Sr(2)	3.5566(4)
Sr(1)···Sr(3)	3.6273(5)	Sr(1)···Sr(2)	3.6298(6)	Sr(1)···Sr(3)	3.6067(4)
Sr(1)···Sr(2)	3.0468(5)	Sr(2)···Sr(3)	3.6604(6)	Sr(2)···Sr(3)	3.9997(4)

ligands show a bond length of 2.464(3) Å. The bonds connecting strontium and methoxy oxygen atoms were 2.669(3) Å (Sr2–O8) and 2.615(3) Å (Sr3–O12), in length.

The crystal structure of **4** is identical to that of **2**, but has fewer intramolecular steric interactions owing to the absence of amine groups in the memp ligand. The Sr–O bonds with μ_3-O atoms show an average length of 2.5446(19) Å. The Sr–O bonds with non-bridging oxygen atoms of the tmhd ligands show a bond length of 2.476(2) Å. The bonds involving tmhd/memp μ_2-O atoms are Sr1–O1 (2.6295(19) Å), Sr3–O1 (2.571(2) Å), Sr1–O3 (2.4244(19) Å), and Sr2–O3 (2.399(2) Å). The bonds between strontium and methoxy oxygen atoms display lengths of 2.704(2) (Sr1–O5), 2.749(2) (Sr2–O10), and 2.730(2) Å (Sr3–O15).

The structural analyses of complexes **5–7** (Fig. S1 (**5**), S2 (**6**)† and Fig. 4 (**7**)) demonstrated the formation of dimers quite similar to those reported for complex **8**. This shows that the introduction of bulkier substituents on the amine or on the alkoxy carbon of these aminoalkoxide ligands does not produce monomeric structures and the complexes stick to a stable dimeric form. Previous attempts to synthesize monomeric [Sr(aminoalkoxide)(tmhd)] by introducing bulky substituents on the ligands have been made; however here we tried to introduce an ethyl group to the amine nitrogen next to the bridging alkoxy groups (in **5**) and two different alkyl groups to the alkoxy carbon (in **6**), where the steric interactions may play an important role in the structure. The strontium ions in these complexes exhibit a distorted octahedral geometry with one aminoalkoxide and one β-diketonate ligand bonded to each strontium ion and the alkoxide oxygen undergoes μ_2-O bridging between strontium ions to complete the hexa-coordinate environment for each metal center. The Sr···Sr nonbonding distances in complexes **5–7** (Table 4) were 3.7183(4), 3.6350(6), and 3.7100(9) Å, respectively. These inter-metal distances were longer than those of the tri-bridged metal pairs and shorter than those of the di-bridged metal pairs in trimeric complexes **2–4**, but in the ranges reported for other dimeric complexes of this class.[4,5] In complex **5**, the average Sr–O and Sr–N bond lengths were 2.5217(17) and 2.7845(2) Å, respectively, which were marginally longer than those in **6**, where the average Sr–O and Sr–N bond lengths were 2.4264(2) and 2.734(3) Å, respectively, and **7**, with average bond lengths of 2.4236(3) Å (Sr–O) and 2.735(5) Å (Sr–N). The bridging angles (Sr–O–Sr) in **5** and **7** were 100.87(6)° and 100.67(12)°, respectively, whereas that in **6** was narrower at 97.17(8)°.

Complex **7**, where the strontium is coordinated to aminoalkoxide ligand dmaemamp and β-diketonate ligand dmhd, and complex **8** are structural isomers. Their structural features are nearly identical; they have dimeric structures, similar average bond lengths (the average Sr–O and Sr–N bond lengths in **8** are (2.430(2) Å) and Sr–N (2.745(3) Å), respectively), and similar Sr···Sr distances of 3.7100(9) Å for **7** and 3.7119(6) Å for **8**.

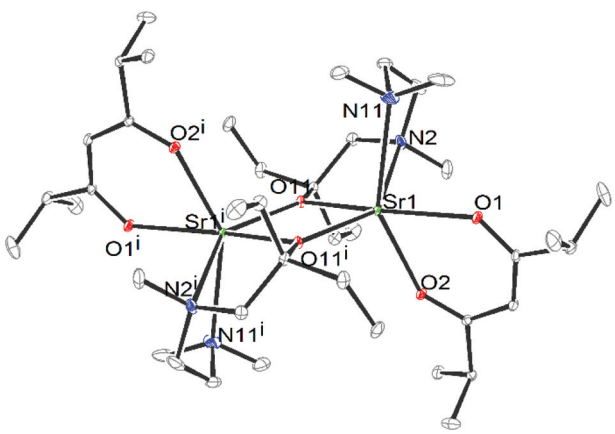

Fig. 4 ORTEP diagram for complex **7**.

NMR

The recorded ^{1}H NMR spectra of complexes **1–7** at room temperature generally exhibited broader peaks, especially for the aminoalkoxide/alkoxide ligands which made the identification of individual peaks difficult. The tmhd/dmhd protons in the spectra displayed comparatively sharper and more identifiable peaks. The broad peaks in the spectra of these complexes may be due to the slow site exchanges in solution at the NMR time scale. In complex **1**, the ^{t}Bu protons from the three tmhd groups exhibited two broad peaks at δ = 1.32 and 1.41 ppm in a 4 : 2 ratio, whereas the β-C*H* protons appeared as a single broad peak with two shoulders at 5.82 ppm. This observation supports the assumption that **1** might have formed a trimer similarly to complexes **2** and **3**. In complex **2**, the ^{t}Bu protons from the three tmhd groups appeared as three distinct peaks at δ = 1.32, 1.34, and 1.39 ppm in a 2 : 3 : 1 ratio and the three β-C*H* protons appeared at δ = 5.83, 5.85, and 5.87 ppm in a 3 : 2 : 1 ratio. The spectrum of **3** showed two peaks for the ^{t}Bu protons one at 1.32 ppm, which was broader and had a shoulder on one side, and another at 1.37 ppm in a 3 : 3 ratio. The β-C*H* protons followed the same pattern showing one broad peak at 5.87 ppm and another at 5.88 ppm. The spectrum of complex **4**, where the less bulky alkoxyalkoxides were the co-ligands with tmhd, showed singlet peaks for the tmhd ^{t}Bu protons at 1.34 ppm and β-C*H* protons at 5.84 ppm. The room-temperature NMR spectra of complexes **1–3** pointed towards free site exchange interactions of ligands in solution, resulting in the formation of the structural isomers. The distinct peaks of complexes **1–3** compared to those of **4** can be related to the speed of these exchange reactions. In the first three complexes, these changes must be faster than those in **4**, where they are slower with respect to the NMR time scale and thus the peak appeared as a broad singlet.

For dimeric complexes **5** and **6**, the tmhd ^{t}Bu protons appeared at δ = 1.35 and 1.34 ppm and the β-C*H* protons at 5.86 and 5.86 ppm, respectively. For complex **7**, the ^{i}Pr protons appeared as a doublet at 1.23 ppm, and β-C*H* protons appeared at 5.46 ppm. These broad peaks for β-diketonates in dimeric complexes indicated slow-paced site exchanges in their solution phase compared to those of trimeric complexes.

Table 4 Selected bond lengths (Å) and bond angles (°) for **5**, **6**, and **7**

[Sr(dmaeeamp)[(tmhd)]$_2$ (**5**)		[Sr(dmaemamb)(tmhd)]$_2$ (**6**)		[Sr(dmaemamp)(tmpd)]$_2$ (**7**)	
Bond lengths (Å)					
Sr(1)–O(3)i	2.3854(16)	Sr(1)–O(3)i	2.387(2)	Sr(1)–O(11)i	2.379(3)
Sr(1)–O(1)	2.4354(18)	Sr(1)–O(1)	2.439(2)	Sr(1)–O(11)	2.438(3)
Sr(1)–O(3)	2.4377(17)	Sr(1)–O(2)	2.460(2)	Sr(1)–O(2)	2.447(3)
Sr(1)–O(2)	2.4430(17)	Sr(1)–O(3)	2.460(2)	Sr(1)–O(1)	2.471(3)
Sr(1)–N(1)	2.748(2)	Sr(1)–N(2)	2.701(3)	Sr(1)–N(2)	2.707(4)
Sr(1)–N(2)	2.821(2)	Sr(1)–N(1)	2.767(3)	Sr(1)–N(11)	2.744(4)
Sr(1)i–O(3)	2.3853(16)	Sr(1)i–O(3)	2.386(2)	Sr(1)i–O(11)	2.379(3)
Sr(1)···Sr(1)i	3.7183(4)	Sr(1)···Sr(1)i	3.6350(6)	Sr(1)···Sr(1)i	3.7099(7)
Bond angles (°)					
O(3)i–Sr(1)–O(1)	112.30(6)	O(3)i–Sr(1)–O(1)	110.70(8)	O(11)i–Sr(1)–O(11)	79.28(10)
O(3)i–Sr(1)–O(3)	79.13(6)	O(3)i–Sr(1)–O(2)	126.14(8)	O(11)i–Sr(1)–O(2)	106.89(10)
O(1)–Sr(1)–O(3)	165.28(6)	O(1)–Sr(1)–O(2)	70.83(8)	O(11)–Sr(1)–O(2)	98.22(10)
O(3)i–Sr(1)–O(2)	113.06(6)	O(3)i–Sr(1)–O(3)	82.83(8)	O(11)i–Sr(1)–O(1)	119.59(10)
O(1)–Sr(1)–O(2)	70.66(6)	O(1)–Sr(1)–O(3)	101.32(8)	O(11)–Sr(1)–O(1)	160.11(10)
O(3)–Sr(1)–O(2)	96.68(6)	O(2)–Sr(1)–O(3)	151.03(8)	O(2)–Sr(1)–O(1)	71.39(10)
O(3)i–Sr(1)–N(1)	94.15(6)	O(3)i–Sr(1)–N(2)	144.61(8)	O(11)i–Sr(1)–N(2)	141.30(11)
O(1)–Sr(1)–N(1)	86.65(6)	O(1)–Sr(1)–N(2)	94.87(9)	O(11)–Sr(1)–N(2)	67.00(11)
O(3)–Sr(1)–N(1)	102.18(6)	O(2)–Sr(1)–N(2)	84.56(9)	O(2)–Sr(1)–N(2)	96.53(12)
O(2)–Sr(1)–N(1)	149.41(6)	O(3)–Sr(1)–N(2)	68.03(8)	O(1)–Sr(1)–N(2)	96.72(12)
O(3)i–Sr(1)–N(2)	135.05(6)	O(3)i–Sr(1)–N(1)	94.07(8)	O(11)i–Sr(1)–N(11)	102.87(13)
O(1)–Sr(1)–N(2)	106.92(6)	O(1)–Sr(1)–N(1)	153.49(9)	O(11)–Sr(1)–N(11)	100.40(14)
O(3)–Sr(1)–N(2)	66.95(6)	O(2)–Sr(1)–N(1)	87.18(8)	O(2)–Sr(1)–N(11)	147.28(14)
O(2)–Sr(1)–N(2)	99.81(6)	O(3)–Sr(1)–N(1)	90.73(8)	O(1)–Sr(1)–N(11)	82.34(14)
N(1)–Sr(1)–N(2)	66.74(6)	N(2)–Sr(1)–N(1)	67.69(9)	N(2)–Sr(1)–N(11)	66.96(16)
Sr(1)i–O(3)–Sr(1)	100.87(6)	Sr(1)i–O(3)–Sr(1)	97.17(8)	Sr(1)i–O(11)–Sr(1)	100.72(10)

VT-NMR

To get a more detailed view of their structures in solution, the NMR spectra of complexes **1–7** (Fig. S3†) were analyzed at low temperatures with toluene-d_8 as the solvent and reference. The low-temperature measurement was expected to give a clearer view of the structures as site exchange interactions will be limited at lower temperatures. The NMR spectrum of complex **1** at 213 K showed one singlet peak for each tmhd ^{t}Bu group at δ = 1.18, 1.22, 1.29, 1.37, 1.47, and 1.50 ppm and three individual peaks for β-C*H* protons at δ = 5.62, 5.84, and 5.99 ppm. This observation of six environmentally different ^{t}Bu groups and three β-C*H* protons supports its trimeric structure and confirms its structural stability in solution. The spectrum of complex **2** exhibited twelve individual singlets for ^{t}Bu groups and six singlets for β-C*H* protons at 213 K. This suggests the existence of two closely related structural isomers at this temperature, and the μ_2-bridging of only one of the six tmhd oxygen atoms can produce a closely related structural isomer with site exchange interactions in solution for this complex. The ^{t}Bu protons in **3** appeared as six singlets at δ = 1.25, 1.27, 1.29, 1.37, 1.38 and 1.44 ppm, and three peaks for β-C*H* protons appeared at δ = 5.76, 5.90, and 5.98 ppm. These peaks for tmhd protons in **3** are broader than those observed for **1** and exhibited shoulders, which indicate the presence of closely related structural isomers in solution. The spectrum of complex **4**, which displayed a single peak at room temperature for the ^{t}Bu protons exhibited four broad peaks for six ^{t}Bu protons at 213 K. These appeared at δ = 1.13 (9H), 1.26 (9H), 1.32 (27H), and 1.47 (9H) ppm; the β-C*H* protons appeared at δ = 5.67 (1H), 5.85 (1H), and 5.98 (1H) ppm.

In the spectrum of dimeric complex **5**, the tmhd proton peaks did not show any changes in their characteristics and remained as singlets for both the ^{t}Bu protons and β-C*H* protons even at 213 K. For complex **6** at 213 K, the ^{t}Bu protons from two tmhd ligands appeared as three peaks at δ = 1.33 (9H), 1.34 (18H), and 1.34 (9H) ppm and the β-C*H* protons appear at δ = 5.88 (0.5H), 5.89 (1H), and 5.91 (0.5H) ppm. The results indicate retention of the dimeric structure in solution with two possible structural isomeric forms coexisting in nearly equal proportions. We suggest that the isomers may be a form of *cis–trans* isomers, where the *trans* form exists in the crystal form and a *cis* form with both tmhd ligands on the same side of the dimer is the other. The spectrum of complex **7** at 253 K displayed two sets of two doublets each with a 2 : 1 ratio, which was again an indication of the presence of two isomers at that temperature. The first set for the major isomer, (which may be the stable *trans* form), appeared as two doublets at δ = 1.18 and 1.19 ppm and a second set of doublets for the minor isomer (*cis* form) appeared at δ = 1.21 and 1.22 ppm. The β-C*H* protons appeared as a singlet peak at 5.40 ppm. However in the spectrum at 213 K, the β-C*H* protons of the two isomers separated and existed as two singlets at δ = 5.50 and 5.52 ppm with a 1 : 2 ratio. The spectral data obtained for the above four trimeric complexes and three dimeric complexes differed according to their structural features and ability to undergo site exchanges in solution at a particular temperature and pace at the NMR time scale.

Mass spectra of complexes **1–6** display dominant peaks at m/z = 725 and 271 which correspond to the $[Sr_2(tmhd)_3]^+$ and $[Sr(tmhd)]^+$ species whereas, complex **7** displays peaks at m/z = 641 ($[Sr_2(dmhd)_3]^+$) and 243 ($[Sr(dmhd)]^+$). The formation of $[Sr_2(tmhd)_3]^+$ and $[Sr(tmhd)]^+$ type fragments during the mass spectroscopic analysis of alkaline earth metal complexes that contain tmhd has been reported earlier. The reason for the fragmentation has been described as a result of ion–molecule reactions in the mass spectrometer source.[9] In the elemental analyses of the complexes, complexes **4** and **6** show considerable deviation from the calculated values even with our best efforts and repeated experiments. All other complexes yielded comparable values with those of the calculated ones. The sensitive nature of the complexes towards air and moisture has an effect on the analyses where complete inertness could not be assured. FT-IR spectra of the complexes display characteristic peaks for this class of complexes. The absence of any –OH peaks confirmed complete reaction and any free ligand presence. The sharp peaks displayed by the complexes around 470 cm^{-1} confirm the diketonate-O–Sr bond formation.[10] Apart from the fragmentation in mass spectra, and elemental analyses where the high sensitivity of the complexes affected the results, the FT-NMR and FT-IR data proved the purity of the bulk samples with no evidence of unreacted reagents, side products or fragmentation.

Thermogravimetric analyses

Thermogravimetric analyses (TGA) of complexes **1–7** were conducted from room temperature to 800 °C under a constant flow of argon. TGA plots of the complexes display a 1–2% mass loss up to 75 °C owing to the evaporation of any trapped solvents in the samples. Complexes **1–4** showed similar characters in their TGA plots (Fig. 5), which demonstrated three-step mass losses. In the first step between 75 and 300 °C, there were mass losses of 30%, 34%, 26%, and 12%, respectively. In the second step, in the 300–370 °C temperature range, the observed mass losses were 40%, 34%, 41%, and 43% respectively. In the final step in the 370–550 °C range further mass losses of 4%, 8%, 7%, and 11% and residual masses of 25%, 21%, 24%, and 31%, respectively, were observed. The first two steps with major mass losses at 75–300 °C and 300–370 °C might be due to the partial evaporation of the complexes and possible fragmentation of the complexes. The final step, with relatively small losses can be attributed to the evaporation of the portions of the decomposed products.

The TGA plots of compounds **5–7** displayed multiple steps (Fig. 6). The complexes showed initial losses of 3% at 90 °C, and then 25% each for **5** and **7** and 30% for **6** up to 250 °C. Further mass losses were observed for complexes **5** and **6** in multiple steps from 250 to 500 °C, with mass losses of 48% for **5** and 45% for **6**. In the case of complex **7**, a 20% mass loss in the second step from 250 to 335 °C and a 19% mass reduction in the third step from 335 to 500 °C were observed. All complexes (**1–7**) displayed high nonvolatile residual masses of 25%, 21%, 24%, 31%, 24%, 21%, and 29%, respectively, reflecting the decomposition of the compounds during the experiments and, thus the temperature instability. As all the sample preparations and the experiments were performed under an air-free atmosphere, the final residue obtained ought to be a mixture of nonvolatile fractions from ligand decomposition and strontium oxide. The calculations based on molecular weight and percentage of strontium in complex **1** show the possible formation of Sr, SrO, and $SrCO_3$ from the decomposition as 20%, 24%, and 34%, respectively. The experimental observation of 25% of the final residue in TGA closely matches with the calculated SrO percentage. However, in other complexes, the possible SrO and $SrCO_3$ percentages were calculated as 23% & 33% (**2**), 23% & 32% (**3**), 25% & 35% (**4**), 23% & 32% (**5**), 23% & 32% (**6**), and 23% & 33% (**7**) showing that the residues are possibly a mixture of strontium oxide and ligand fractions. To prove the above calculations, X-ray diffraction analysis on the residual powder of **1** was con-

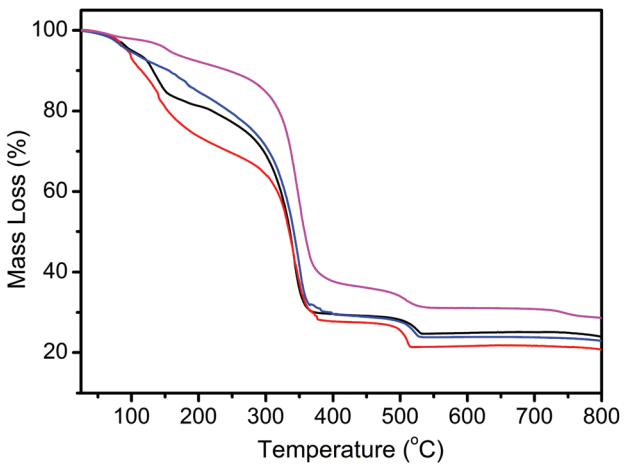

Fig. 5 TGA plot of complexes **1** (black), **2** (red), **3** (blue), and **4** (violet).

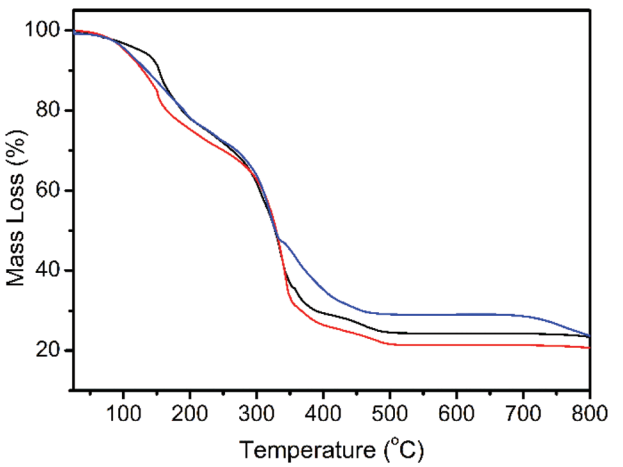

Fig. 6 TGA plot of complexes **5** (black), **6** (red), and **7** (blue).

ducted. The peaks obtained from the experiment (Fig. S4†) agree with the formation of SrO from the decomposition, and show no evidence for the presence of $SrCO_3$.

The study of the volatile character of the complexes was conducted under reduced pressure (10^{-6} Torr) at room temperature. The experiment resulted in the decomposition of complexes **1** and **2** at 170 °C, whereas all other complexes (**3–7**) displayed a stable character throughout the experiment.

Experimental

NMR spectra were recorded on a Bruker 300 MHz spectrometer with C_6D_6 as the solvent and standard. IR spectra were obtained with a Nicolet Nexus FT-IR spectrophotometer. Elemental analyses were carried out on a ThermoScientific OEA Flash 2000 analyzer. Thermo-gravimetric analyses were conducted on a SETARAM 92-18 TG-DTA instrument with a constant flow of nitrogen throughout the experiment. $(Sr(btsa)_2{\cdot}2DME)$,[8] and the aminoalcohols, memampH,[5] emeampH,[5] imeampH,[5] mempH,[11] dmaeeampH,[5] dmaemambH[5] and dmaemampH[5] were prepared by modified literature methods. All reactions except ligand preparations were carried out under inert dry conditions using standard Schlenk techniques or in an argon-filled glove box. Hexane and toluene were purified with an Innovative Technology PS-MD-4 solvent purification system. 2,2-Dimethyloxirane was purchased from TCI, and all other chemicals were purchased from Aldrich and used as received.

Syntheses

General procedure for the synthesis of aminoalcohols. Isobutylene oxide was added dropwise at 0 °C with constant stirring to a 40% water solution of the corresponding amine in a three-necked flask fitted with a reflux condenser. After the addition, the reaction mixture was warmed to room temperature and stirring was continued for another 6 h. Then, the product was extracted with diethyl ether three times (3 × 50 mL), and the combined organic layer was washed with brine. The solvent was removed, and the crude product was distilled to obtain the pure product.

1-((2-Methoxyethyl)(methyl)amino)-2-methylpropan-2-ol (memampH). Isobutylene oxide (7.21 g, 0.1 mol), and 2-methoxy-*N*-methylethan-1-amine (8.91 g, 0.1 mol) were used. Bp 60 °C/0.5 Torr; yield 11.6 g (72%). FTIR (ν_{max}/cm^{-1}) 3463 (OH). ^{1}H NMR (C_6D_6, 300 MHz): δ_H 1.18 (6H, s, C(C*H*$_3$)O), 2.18 (2H, s, C*H*$_2$C(CH$_3$)$_2$), 2.20 (3H, s, N(C*H*$_3$)), 2.51 (2H, t, CH$_3$OCH$_2$C*H*$_2$), 3.10 (3H, s, C*H*$_3$O), 3.14 (2H, t, CH$_3$OC*H*$_2$CH$_2$), 3.44 (1H, s, O*H*). Anal. Calcd for $C_8H_{19}NO_2$: C, 59.59; H, 11.88; N, 8.69. Found: C, 59.54; H, 11.86; N, 8.65.

1-(Ethyl(2-methoxyethyl)amino)-2-methylpropan-2-ol (emeampH). Isobutylene oxide (7.21 g, 0.1 mol), and *N*-ethyl-2-methoxyethan-1-amine (10.3 g, 0.1 mol) were used. Bp 60 °C/0.5 Torr; yield 14.0 g (80%). FTIR (ν_{max}/cm^{-1}) 3458 (OH). ^{1}H NMR (C_6D_6, 300 MHz): δ_H 0.87 (3H, t, N(CH$_2$C*H*$_3$)), 1.20 (6H, s, C(C*H*$_3$)O), 2.24 (2H, s, C*H*$_2$C(CH$_3$)$_2$), 2.42 (2H, q, N(C*H*$_2$CH$_3$)), 2.58 (2H, t, CH$_3$OCH$_2$C*H*$_2$), 3.06 (3H, s, C*H*$_3$O), 3.15 (2H, t, CH$_3$OC*H*$_2$CH$_2$), 3.63 (1H, s, O*H*). Anal. Calcd for $C_9H_{21}NO_2$: C, 61.67; H, 12.08; N, 7.99. Found: C, 61.48; H, 11.98; N, 7.92.

1-(Isopropyl(2-methoxyethyl)amino)-2-methylpropan-2-ol (imeampH). Isobutylene oxide (7.21 g, 0.1 mol) and *N*-(2-methoxyethyl)propan-2-amine (11.7 g, 0.1 mol) were used. Bp 75 °C/0.5 Torr; yield 10.9 g (58%). FTIR (ν_{max}/cm^{-1}) 3457 (OH). ^{1}H NMR (C_6D_6, 300 MHz): δ_H 0.84 (6H, d, N(CH(C*H*$_3$)$_2$)), 1.23 (6H, s, C(C*H*$_3$)O), 2.23 (2H, s, C*H*$_2$C(CH$_3$)$_2$), 2.53 (2H, t, CH$_3$OCH$_2$C*H*$_2$), 2.66 (1H, m, N(C*H*(CH$_3$)$_2$)), 3.07 (3H, s, C*H*$_3$O), 3.16 (2H, t, CH$_3$OC*H*$_2$CH$_2$), 3.89 (1H, s, O*H*). Anal. Calcd for $C_{10}H_{23}NO_2$: C, 63.45; H, 12.25; N, 7.40. Found: C, 63.21; H, 11.98; N, 7.28.

1-((2-(Dimethylamino)ethyl)(ethyl)amino)-2-methylpropan-2-ol (dmaeeampH). Isobutylene oxide (7.21 g, 0.1 mol) and *N*1-ethyl-*N*2,*N*2-dimethylethane-1,2-diamine (11.6 g, 0.1 mol) were used. Bp 60 °C/0.5 Torr; yield 14.5 g (77%). FTIR (ν_{max}/cm^{-1}) 3378 (OH). ^{1}H NMR (C_6D_6, 300 MHz): δ_H 0.88 (3H, t, N(CH$_2$C*H*$_3$)), 1.26 (6H, s, C(C*H*$_3$)O), 2.02 (6H, s, N(C*H*$_3$)$_2$), 2.12 (2H, t, (CH$_3$)$_2$NCH$_2$C*H*$_2$), 2.26 (2H, s, C*H*$_2$C(CH$_3$)$_2$), 2.33 (2H, t, (CH$_3$)$_2$NC*H*$_2$CH$_2$), 2.44 (2H, q, N(C*H*$_2$CH$_3$)), 5.86 (1H, s, O*H*). Anal. Calcd for $C_{10}H_{24}N_2O$: C, 63.78; H, 12.85; N, 14.88. Found: C, 63.47; H, 12.79; N, 14.79.

1-((2-(Dimethylamino)ethyl)(methyl)amino)-2-methylbutan-2-ol (dmaemambH). 2-Ethyl-2-methyl-oxirane (0.860 g, 0.1 mol) and *N*,*N*,*N*′-trimethylethylenediamine (10.2 g, 0.1 mol) were used. Bp 80 °C/0.05 Torr; yield 12.3 g, 65%. FTIR (ν_{max}/cm^{-1}) 3209 (OH). ^{1}H NMR (C_6D_6, 300 MHz): δ_H 0.90 (3H, t, C(CH$_3$)(CH$_2$C*H*$_3$)O), 1.07 (3H, s, C(C*H*$_3$)(CH$_2$CH$_3$)O), 1.45 (2H, m, C(CH$_3$)(C*H*$_2$CH$_3$)O), 2.23 (6H, s, N(C*H*$_3$)$_2$), 2.35 (4H, m, N(CH$_3$)$_2$C*H*$_2$C*H*$_2$), 2.40 (3H, s, CH$_2$N(C*H*$_3$)CH$_2$), 2.55 (2H, m, N(CH$_3$)C*H*$_2$), 5.78 (1H, s, O*H*). Anal. Calcd for $C_{10}H_{24}N_2O$: C, 63.78; H, 12.85; N, 14.88. Found: C, 63.42; H, 12.80; N, 14.20.

1-(2-Methoxyethoxy)-2-methylpropan-2-ol (mempH). 2-Methoxyethanol (7.61 g, 0.1 mol) was added dropwise at 0 °C with constant stirring to a suspension of sodium hydride (2.40 g, 0.1 mol) in THF. The mixture was then allowed to reach room temperature and stirring was continued for another 30 min. Isobutylene oxide (10.8 g, 0.2 mol) was added dropwise to the above mixture at 0 °C. The reaction mixture was slowly heated to 90 °C and stirring was continued for another 12 h. After cooling to room temperature the reaction was quenched with ammonium chloride solution at 0 °C. The product was extracted with ethyl acetate (3 × 50 mL), and the combined organic layer was washed with brine. The solvent was removed, and the crude product was distilled (60 °C/0.05 Torr) to obtain the product as a colorless liquid (6.70 g, 45%). FTIR (ν_{max}/cm^{-1}) 3450 (OH). ^{1}H NMR (C_6D_6, 300 MHz): δ_H 1.18 (6H, s, C(C*H*$_3$)$_2$O), 2.48 (1H, s, O*H*), 3.07 (3H, s, C*H*$_3$OCH$_2$), 3.11 (2H, s, CH$_2$CH$_2$OC*H*$_2$), 3.23 (2H, t, CH$_2$C*H*$_2$OCH$_2$), 3.40 (2H, t, CH$_3$OC*H*$_2$CH$_2$). Anal. Calcd for $C_7H_{16}O_3$; C, 56.73; H, 10.88. Found: C, 56.58; H, 10.80.

General procedure for [Sr(R-O)(β-diketonate)]$_x$ complexes. The aminoalcohol/alkoxyalcohol in toluene (5 mL) was added dropwise at room temperature to a solution of Sr(btsa)2·2DME in toluene (15 mL) with stirring. After stirring for 5 h at room

temperature, 2,2,6,6-tetramethyl-3,5-heptanedione (tmhdH) or 2,6-dimethyl-3,5-heptanedione (dmhdH) was added to the reaction mixture, which was then stirred for another 15 h at room temperature. Then, the solvent was evaporated and the residue was extracted with hexane, filtered, and dried to obtain the product. X-ray quality crystals were grown from concentrated hexane solutions upon cooling.

*[Sr(memamp)(tmhd)]$_3$ (**1**).* Sr(btsa)$_2$·2DME (0.590 g, 1.0 mmol), 1-((2-methoxyethyl)(methyl)amino)-2-methylpropan-2-ol (memampH) (0.161 g, 1.0 mmol), and 2,2,6,6-tetramethyl-3,5-heptanedione (tmhdH) (0.184 g, 1.0 mmol) were used. Yield 0.384 g (89%). M.p. 181 °C. FTIR (ν_{max}/cm^{-1}) 2950m, 2867w, 1599s, 1577m, 1533w, 1503w, 1452m, 1423vs, 1357w, 1209w, 1126w, 1106w, 1036w, 863w, 470w. ^{1}H NMR (C_6D_6, 300 MHz): δ_H 1.32 (36H, br, C(C*H*$_3$)$_3$), 1.41 (18H, br, C(C*H*$_3$)$_3$), 1.42–1.90 (18H, broad peaks, C(C*H*$_3$)$_2$O), 1.92–3.40 (36H, br) 5.82 (3H, br, β-C*H*). Anal. Calcd for $C_{57}H_{111}N_3O_{12}Sr_3$: C, 52.93; H, 8.65; N, 3.25. Found: C, 52.60; H, 8.62; N, 3.23. MS: *m*/*z* calcd for [Sr(memamp)(tmhd)]$_3$: 1293.53 [M]$^+$; found 726 [Sr$_2$(tmhd)$_3$]$^+$, 271 [Sr(tmhd)]$^+$.

*[Sr(emeamp)(tmhd)]$_3$ (**2**).* Sr(btsa)$_2$·2DME (0.590 g, 1.0 mmol), 1-(ethyl(2-methoxyethyl)amino)-2-methylpropan-2-ol (emeampH) (0.175 g, 1.0 mmol), and 2,2,6,6-tetramethyl-3,5-heptanedione (tmhdH) (0.184 g, 1.0 mmol) were used. Yield 0.382 g (86%). M.p. 178 °C. FTIR (ν_{max}/cm^{-1}) 2951m, 1599s, 1577m, 1533w, 1504w, 1452m, 1421vs, 1387w, 1358w, 1221w, 1181w, 1125w, 1056w, 973w, 863w, 471w. ^{1}H NMR (C_6D_6, 300 MHz): δ_H 0.92 (9H, t, br, NCH$_2$C*H*$_3$), 1.32 (18H, s, br, C(C*H*$_3$)$_3$), 1.34 (27H, s, br, C(C*H*$_3$)$_3$), 1.39 (9H, s, br, C(C*H*$_3$)$_3$), 1.57–1.80 (18H, broad peaks, C(C*H*$_3$)$_2$O), 2.32–3.40 (33H, br), 5.83, 5.85 & 5.87 (3H, br, β-C*H*). Anal. Calcd for $C_{60}H_{117}N_3O_{12}Sr_3$: C, 53.96; H, 8.83; N, 3.15. Found: C, 53.24; H, 8.73; N, 3.07. MS: *m*/*z* calcd for [Sr(emeamp)(tmhd)]$_3$: 1335.58 [M]$^+$; found 726 [Sr$_2$(tmhd)$_3$]$^+$, 271 [Sr(tmhd)]$^+$.

*[Sr(imeamp)(tmhd)]$_3$ (**3**).* Sr(btsa)$_2$·2DME (0.590 g, 1.0 mmol), 1-(isopropyl(2-methoxyethyl)amino)-2-methylpropan-2-ol (imeampH) (0.189 g, 1.0 mmol), and 2,2,6,6-tetramethyl-3,5-heptanedione (tmhdH) (0.184 g, 1.0 mmol) were used. Yield 0.367 g (80%). M.p. 111 °C. FTIR (ν_{max}/cm^{-1}) 2964m, 2870w, 1593s, 1576m, 1534w, 1504w, 1452m, 1417vs, 1358w, 1127w, 990w, 863w, 473w. ^{1}H NMR (C_6D_6, 300 MHz): δ_H 0.70–1.10 (18H, br, CH(C*H*$_3$)$_2$) 1.32 (27H, s, br, C(C*H*$_3$)$_3$), 1.37 (27H, s, C(C*H*$_3$)$_3$), 1.64 (18H, broad peaks, C(C*H*$_3$)$_2$O), 3.04 (3H, m, C*H*(CH$_3$)$_2$), 2.10–3.50 (30H, br), 5.87 (1.5H, s, br, β-C*H*), 5.88 (1.5H, s, br, β-C*H*). Anal. Calcd for $C_{63}H_{123}N_3O_{12}Sr_3$: C, 54.93; H, 9.00; N, 3.05. Found: C, 54.27; H, 8.98; N, 3.03. MS: *m*/*z* calcd for [Sr(imeamp)(tmhd)]$_3$: 1377.5 [M]$^+$; found 726 [Sr$_2$(tmhd)$_3$]$^+$, 271 [Sr(tmhd)]$^+$.

*[Sr(memp)(tmhd)]$_3$ (**4**).* Sr(btsa)$_2$·2DME (0.590 g, 1.0 mmol), 1-(2-methoxyethoxy)-2-methylpropan-2-ol (mempH) (0.148 g, 1.0 mmol), and 2,2,6,6-tetramethyl-3,5-heptanedione (tmhdH) (0.184 g, 1.0 mmol) were used. Yield 0.368 g (88%). M.p. 93 °C. FTIR (ν_{max}/cm^{-1}) 2950m, 2866w, 1598s, 1576w, 1533w, 1503w, 1455m, 1419vs, 1358w, 1224w, 1182w, 1127w, 1084w, 950w, 863w, 471w. ^{1}H NMR (C_6D_6, 300 MHz): δ_H 1.34 (54H, s, C(C*H*$_3$)$_3$), 1.61 (18H, s, br, C(C*H*$_3$)$_2$O), 3.13 (15H, s, br, C*H*$_3$O & C*H*$_2$(CH$_3$)$_2$O), 3.30 (6H, s, br, CH$_3$OCH$_2$C*H*$_2$), 3.37 (6H, s, CH$_3$OC*H*$_2$CH$_2$), 5.84 (3H, s, β-C*H*). Anal. Calcd for $C_{57}H_{109}O_{15}Sr_3$: C, 51.71; H, 8.20. Found: C, 50.02; H, 8.13. MS: *m*/*z* calcd for [Sr(memp)(tmhd)]$_3$: 1254.26 [M]$^+$; found 726 [Sr$_2$(tmhd)$_3$]$^+$, 271 [Sr(tmhd)]$^+$.

*[Sr(dmaeeamp)(tmhd)]$_2$ (**5**).* Sr(btsa)$_2$·2DME (0.590 g, 1.0 mmol), 1-((2-(dimethylamino)ethyl)(ethyl)amino)-2-methylpropan-2-ol (dmaeeampH) (0.188 g, 1.0 mmol), and 2,2,6,6-tetramethyl-3,5-heptanedione (tmhdH) (0.184 g, 1.0 mmol) were used. Yield 0.431 g (94%). M.p. 205 °C. FTIR (ν_{max}/cm^{-1}) 2949m, 2862w, 2836w, 1589vs, 1577m, 1535w, 1504w, 1455m, 1418vs, 1387w, 1355w, 1224w, 1184w, 982w, 863w, 470w. ^{1}H NMR (C_6D_6, 300 MHz): δ_H 0.85 (6H, t, NCH$_2$C*H*$_3$), 1.25 (6H, s, br, C(C*H*$_3$)$_2$O), 1.35 (36H, s, C(C*H*$_3$)$_3$), 1.48 (6H, s, br, C(C*H*$_3$)$_2$O), 1.90–2.80 (28H, br), 5.86 (2H, s, β-C*H*). Anal. Calcd for $C_{42}H_{84}N_4O_6Sr_2$: C, 55.05; H, 9.24; N, 6.11. Found: C, 54.82; H, 9.18; N, 6.01. MS: *m*/*z* calcd for [Sr(dmaeeamp)(tmhd)]$_2$: 916.37 [M]$^+$; found 726 [Sr$_2$(tmhd)$_3$]$^+$, 271 [Sr(tmhd)]$^+$.

*[Sr(dmaemamb)(tmhd)]$_2$ (**6**).* Sr(btsa)$_2$·2DME (0.590 g, 1.0 mmol), 1-((2-(dimethylamino)ethyl)(methyl)amino)-2-methylbutan-2-ol (dmaemambH) (0.188 g, 1.0 mmol), and 2,2,6,6-tetramethyl-3,5-heptanedione (tmhdH) (0.184 g, 1.0 mmol) were used. Yield 0.407 g (89%). M.p. 154 °C. FTIR (ν_{max}/cm^{-1}) 2958m, 2862w, 1590s, 1577w, 1535w, 1504w, 1448w, 1419vs, 1356w, 1183w, 1128w, 1020w, 976w, 864w, 470w. ^{1}H NMR (C_6D_6, 300 MHz): δ_H 0.90 (6H, br, C(CH$_3$)(CH$_2$C*H*$_3$)O), 1.15–1.28 (6H, br, C(C*H*$_3$)(CH$_2$CH$_3$)O), 1.34 (36H, s, C(C*H*$_3$)$_3$), 1.41–1.66 (4H, m, br, C(CH$_3$)(C*H*$_2$CH$_3$)O), 1.80–2.70 (30H, br), 5.86 (2H, s, β-C*H*). Anal. Calcd for $C_{42}H_{84}N_4O_6Sr_2$: C, 55.05; H, 9.24; N, 6.11. Found: C, 52.55; H, 9.22; N, 6.05. MS: *m*/*z* calcd for [Sr(dmaemamb)(tmhd)]$_2$: 916.37 [M]$^+$; found 726 [Sr$_2$(tmhd)$_3$]$^+$, 271 [Sr(tmhd)]$^+$.

*[Sr(dmaemamp)(dmhd)]$_2$ (**7**).* Sr(btsa)$_2$·2DME (0.590 g, 1.0 mmol), 3-(((2-(dimethylamino)ethyl)(methyl)amino)-methyl)-pentan-3-ol (dmaemampH) (0.202 g, 1.0 mmol), and 2,6-dimethyl-3,5-heptanedione (dmhdH) (0.156 g, 1.0 mmol) were used. Yield 0.422 g (95%). M.p. 163 °C. FTIR (ν_{max}/cm^{-1}) 2960m, 2926w, 2866w, 1604vs, 1525w, 1500w, 1450s, 1311w, 1167w, 1037w, 784w, 425w. ^{1}H NMR (C_6D_6, 300 MHz): δ_H 0.89 (12H, br, C(CH$_2$C*H*$_3$)$_2$O), 1.23 (24H, d, CH(C*H*$_3$)$_2$), 1.60 (4H, m, br, C*H*(CH$_3$)$_2$), 1.80–2.4 (26H, br), 2.40–2.60 (12H, m, br, C(C*H*$_2$CH$_3$)$_2$O & (CH$_3$)$_2$NC*H*$_2$), 5.46 (2H, s, β-C*H*). Anal. Calcd for $C_{40}H_{80}N_4O_6Sr_2$: C, 54.08; H, 9.08; N, 6.31. Found: C, 53.77; H, 8.89; N, 6.27. MS: *m*/*z* calcd for [Sr(dmaemamp)(dmhd)]$_2$: 888.32 [M]$^+$; found 641 [Sr$_2$(dmhd)$_3$]$^+$, 243 [Sr(dmhd)]$^+$.

X-ray crystallography

Single crystals of all complexes were grown from saturated hexane solutions at −30 °C. A specimen of suitable size and quality was coated with Paratone oil and mounted onto a glass capillary. Reflection data were collected on a Bruker Apex II-CCD area detector diffractometer, with graphite-monochromated MoKα radiation (λ = 0.71073 Å). The hemisphere of reflection data was collected as ω scan frames with 0.3° per frame and an exposure time of 10 s per frame. The SAINT[12] software was used for cell refinement and data deduction. The

data were corrected for Lorentz and polarization effects. An empirical absorption correction was applied using the SADABS program.[13] The structure was solved by direct methods and all non-hydrogen atoms were subjected to anisotropic refinement by full-matrix least-squares on F^2 by using the SHELXTL/PC package.[14] Hydrogen atoms were placed at their geometrically calculated positions and refined riding on the corresponding carbon atoms with isotropic thermal parameters. CCDC 1034384–1034389 for complexes **2–7** contain the supplementary crystallographic data for this paper.

Conclusion

The efforts to synthesize new heteroleptic strontium complexes by introducing a variety of donor-functionalized alkoxide ligands as well as different β-diketonate ligands were successful. The introduction of terminal methoxy groups to the ligands resulted in a decrease in steric effects of the ligands, which led to the formation of trimeric complexes **1–4**. The structures of complexes **2–4** comprised three metal centers connected by two sets of μ_3-O bonding and two sets of μ_2-O bonding. All of the strontium atoms in complexes **2** and **4** were seven-coordinated, whereas in **3** a mixture of six- and seven-coordinated geometry was displayed. Complexes **5–7** displayed dimeric geometry and showed similar structural features to the known heteroleptic dimeric complexes. The attempts to impose structural changes from the dimeric form by introducing ethyl groups on the amine nitrogen and the alkoxy carbon of the aminoalkoxide ligands proved insufficient. VT-NMR studies confirmed the stability of all the complexes in solutions with no evidence of fragmentation. Thermo-gravimetric analyses show major weight losses for all the trimeric and dimeric complexes in two steps in the 75–370 °C region. Complexes **3–7** exhibit good stability at higher temperatures in sublimation studies, and studies for the possible application of these heteroleptic strontium complexes as potential precursors for the growth of thin films of $SrTiO_3$ (STO) and $Ba_{0.5}Sr_{0.5}TiO_3$ (BSTO) are examined. Besides that, the high solubility of these complexes in a variety of organic solvents makes them highly suitable for the synthesis of STO nanoparticles in the solution phase.

Acknowledgements

We would like to thank the Center for Chemical Analysis at the Korea Research Institute of Chemical Technology (KRICT) for allowing the use of their facilities and Bruker SMART APEX II for solving the molecular structures. This research was supported by the Converging Research Center Program through the Ministry of Education, Science and Technology (2013K000153).

Notes and references

1 (*a*) S. Ezhilvalavan and T. Y. Tseng, *Mater. Chem. Phys.*, 2000, **65**, 227; (*b*) A. C. Jones and P. R. Chalker, *J. Phys. D: Appl. Phys.*, 2003, **36**, R80; (*c*) Z. X. Shen and D. S. Dessau, *Phys. Rep.*, 1995, **253**, 1; (*d*) H. Heikkinen, L. S. Johansson, E. Nykanen and L. Niinisto, *Appl. Surf. Sci.*, 1998, **133**, 205; (*e*) K. D. Kreuer, *Annu. Rev. Mater. Res.*, 2003, **33**, 333; (*f*) M. Mogensen and S. Skaarup, *Solid State Ionics*, 1996, **86–88**, 1151.

2 (*a*) O. S. Kwon, S. K. Kim, M. Cho, C. S. Hwang and J. Jeong, *J. Electrochem. Soc.*, 2005, **152**, C229; (*b*) R. A. Gardiner, D. C. Gordon, G. T. Stauf and B. A. Vaartstra, *Chem. Mater.*, 1994, **6**, 1967; (*c*) S. R. Drake, S. A. S. Miller and D. J. Williams, *Inorg. Chem.*, 1993, **32**, 3227; (*d*) T. Hatanpää, M. Vehkamäki, I. Mutikainen, J. Kansikas, M. Ritala and M. Leskelä, *Dalton Trans.*, 2004, 1181; (*e*) M. Vehkamäki, T. Hatanpää, T. Hanninen, M. Ritala and M. Leskelä, *Electrochem. Solid-State Lett.*, 1999, **2**, 504; (*f*) T. Hatanpää, M. Ritala and M. Leskelä, *J. Organomet. Chem.*, 2007, **692**, 5256; (*g*) B. Sedai, M. J. Heeg and C. H. Winter, *Organometallics*, 2009, **28**, 1032; (*h*) H. M. El-Kaderi, M. J. Heeg and C. H. Winter, *Organometallics*, 2004, **23**, 4995; (*i*) W. D. Buchanan, M. A. Guino-o and K. Ruhlandt-Senge, *Inorg. Chem.*, 2010, **49**, 7144; (*j*) J. A. T. Norman, M. Perez, M. S. Kim, X. Lei, S. Ivanov, A. Derecskei-Kovacs, L. Matz, I. Buchanan and A. L. Rheingold, *Inorg. Chem.*, 2011, **50**, 12396.

3 (*a*) J. P. Lee, M. H. Park, T.-M. Chung, Y. Kim and M. M. Sung, *Bull. Korean Chem. Soc.*, 2004, **25**, 475; (*b*) S. W. Lee, O. S. Kwon, J. H. Han and C. S. Hwang, *Appl. Phys. Lett.*, 2008, **92**, 222903; (*c*) T. Blanquart, J. Niinistö, M. Gavagnin, V. Longo, V. R. Pallem, C. Dussarrat, M. Ritala and M. Leskela, *Chem. Mater.*, 2012, **24**, 3420; (*d*) J. Niinistö, K. Kukli, M. Kariniemi, M. Ritala, M. Leskelä, N. Blasco, A. Pinchart, C. Lachaud, N. Laaroussi, Z. Wang and C. Dussarrat, *J. Mater. Chem.*, 2008, **18**, 5243; (*e*) S. M. George, B. K. Park, C. G. Kim and T.-M. Chung, *Bull. Korean Chem. Soc.*, 2013, **34**, 967.

4 S. M. George, B. K. Park, C. G. Kim and T.-M. Chung, *Eur. J. Inorg. Chem.*, 2014, 2002.

5 S. M. George, H.-S. Kim, M. S. Lah, B. K. Park, C. G. Kim and T.-M. Chung, *Dalton Trans.*, 2014, **43**, 14461.

6 I. Baxter, J. A. Darr, S. R. Drake, M. B. Hursthouse, K. M. Abdul Malik and D. M. P. Mingos, *J. Chem. Soc., Dalton Trans.*, 1997, 2875.

7 J. Brooks, H. O. Davies, T. J. Leedham, A. C. Jones and A. Steiner, *Chem. Vap. Deposition*, 2000, **6**, 66.

8 M. Westerhausen, *Inorg. Chem.*, 1991, **30**, 96.

9 (*a*) J. R. Majer, in *Mass Spectrometry of Metal Compounds*, ed. J. Charalambous, Butterworth and Co., London, 1975, p. 272; (*b*) S. M. Schildcrout, *Inorg. Chem.*, 1980, **19**, 224; (*c*) S. B. Turnispeed, R. M. Barkley and R. Sievers, *Inorg. Chem.*, 1991, **30**, 1164; (*d*) S. R. Drake, M. B. Hursthouse,

K. M. A. Malik and D. J. Otwaya, *J. Chem. Soc., Dalton Trans.*, 1993, 2883; (*e*) J. Brooks, H. O. Davies, T. J. Leedham, A. C. Jones and A. Steiner, *Chem. Vap. Deposition*, 2000, **6**(2), 66.

10 (*a*) K. Nakamoto and A. E. Martell, *J. Chem. Phys.*, 1960, **32**, 588; (*b*) M. Mikami, I. Nakagawa and T. Shimanouchi, *Spectrochim. Acta, Part A*, 1967, **23**, 1037; (*c*) H.-K. Ryu, J. S. Heo, S.-I. Cho, C. Chung and S. H. Moon, *J. Electrochem. Soc.*, 2000, **147**, 1130.

11 M. Kim, H. S. Jang, T.-M. Chung, C. G. Kim, Y. Kim and B. R. Cho, *Bull. Korean Chem. Soc.*, 2005, **26**, 829.

12 *SAINT, version 5.0, Data integration software*, Bruker AXS Inc., Madison, WI, 1998.

13 G. M. Sheldrick, *SADABS, Program for absorption correction with the Bruker SMART system*, Universitat Gottingen, Germany, 1996.

14 G. M. Sheldrick, *SHELXL-93, Program for the refinement of crystal structures*, Universitat Gottingen, Germany, 1993.